The Effect of α-Actinin on the Length Distribution of F-Actin

D. Biron and E. Moses
Department of Physics of Complex Systems, Weizmann Institute of Science, Rehovot, Israel

ABSTRACT Actin filament length distribution in cells is often regulated to fit specific tasks. In comparison to the well-studied regulation of the average filament length (e.g., using capping proteins), controlling the width of the distribution is less well understood. We utilize two complementary methods to measure the effect of α-actinin on the width of the distribution of lengths of F-actin in vitro. Analyzing transmission electron micrographs shows that crosslinking by α-actinin reduces the width of the length distribution of F-actin, decreasing the coefficient of variation by two- to threefold. Analysis of fluorescence data from depolymerization assays confirms this observation. We suggest a mechanistic molecular model in which a local (weak) stabilization of crosslinked monomers in the filament is the physical origin of the decrease in the variance of lengths. Although α-actinin is known to bind reversibly to F-actin, our model shows that even weak binding can produce this effect, and that in fact it persists throughout a wide range of binding strengths.

INTRODUCTION

Actin polymerization and depolymerization can be controlled by a number of actin binding proteins. Gelsolin, for example, is a well-characterized Ca^{2+}-activated actin binding protein, which severs filaments, caps the plus end, and assists in the formation of polymerization nucleation sites (Kreis and Vale, 1999; Yin, 1999). In general, at steady state each gelsolin molecule is associated with one actin filament, so that controlling the actin-gelsolin stoichiometry regulates the average length of F-actin filaments. Other actin binding proteins affect the F-actin length distribution in a more complex fashion (e.g., talin; see Ruddies et al., 1993).

Crosslinkers are a different type of actin binding protein which are used to control filament organization. The actin crosslinker α-actinin is a rod-shaped antiparallel homodimer (Kreis and Vale, 1999). It has two actin binding sites (at opposing ends of the molecule), typically 30–40-nm apart in high salt concentration. Alpha-actinin weakly contacts two monomers along the long-pitch helix of the actin filament (McGough et al., 1994). As a result, it does not bind to G-actin but binds reversibly (i.e., the bond energy is (2 ± 1) k_BT) to F-actin (Miyata et al., 1996). It is used to orient F-actin in an approximately parallel fashion, e.g., in actin-contracting networks such as muscle fibers or in the contractile ring. Our main result lies in demonstrating that α-actinin also contributes to the regulation of the variance of the lengths of F-actin.

In vitro actin polymerization assays consistently reveal an exponential steady-state distribution of filament lengths both in the absence and in the presence of severing and capping proteins (Xu et al., 1999; Littlefield and Fowler, 1998; Piekenbrock and Sackmann, 1992). The exponential steady-state distribution was theoretically shown to emerge from detailed modeling of actin polymerization and depolymerization dynamics (Edelstein-Keshet and Ermentrout, 1998). We shall also show that it can be derived in a more general mathematical context as a consequence of the fact that monomer exchange is a random process known as an ''homogeneous zero-range process'' (Evans, 2000; see also Materials and Methods, below; and Results, below).

The exponential distribution is wide in the sense that its width (σ_l) is equal to its mean ($\langle l \rangle$). This is measured by the coefficient of variation, defined as $C_\sigma = \sigma_l/\langle l \rangle$, which in the exponential case equals 1. Length distributions in vivo are strikingly different. Cells can optimize filament lengths for specific tasks, resulting in distributions that are much narrower (i.e., $C_\sigma < 1$).

The role of regulating the distribution has also come up in the context of the viscoelastic properties of actin gels. A number of articles have recently dealt with actin rheology, giving conflicting experimental measurements for the values of the elastic constants of the actin gel (Allen et al., 1996; Janmey et al., 1994; Newman et al., 1993). In a article resolving the issue (Xu et al., 1998) the preferred explanation for the apparent contradiction was that the distribution of F-actin length varied between experiments and over time, due to different preparation protocols. The first and second moment, or average length and variance of the distribution, will thus be of major importance also in determining the elastic behavior of the cell.

MATERIALS AND METHODS

Cytoskeletal proteins and buffers

Actin, gelsolin, α-actinin, phalloidin, G-buffer (5 mM Tris pH 8.0, 0.2 mM $CaCl_2$, 0.2 mM ATP), and actin polymerization inducer $10\times$ (500 mM KCl, 50 mM $MgCl_2$, 100 mM ATP) were purchased in lyophilized form from Cytoskeleton (Denver, CO). The buffer used for depolymerization in high KCl concentration (H-buffer) was prepared by dissolving 1 M KCl in $0.4\times$ polymerization buffer. Cofilin was purchased from Molecular Probes (Eugene, OR). Lyophilized proteins were reconstituted according to Cytoskeleton protocols.

Submitted September 9, 2003, and accepted for publication January 2, 2004.

Address reprint requests to David Biron, Weizmann Institute of Science, Physics of Complex Systems, Rehovot 76100 Israel. Tel.: 972-8-934-2662; E-mail: david.biron@weizmann.ac.il.

0006-3495/04/05/3284/07 $2.00

F-actin preparation for transmission electron micrographs

Lyophilized rabbit skeletal muscle actin was polymerized at a concentration of 1 mg/ml according to Cytoskeleton's protocols. Filaments were then stabilized by adding phalloidin at a 1:3 stoichiometry with actin. We checked that nonstabilized samples produce similar distributions to those of stabilized ones.

In samples containing α-actinin, it was added after polymerization reached a steady state at a stoichiometry of 1:5 with actin. The time dependence of the distribution of crosslinked filaments was measured by applying drops of filaments in suspension to transmission electron microscope (TEM) grids at increasing intervals, starting shortly after the addition of α-actinin. Phalloidin was not used in these samples.

Negative staining

F-actin suspension (1.0 mg/ml) was diluted to an actin concentration of ~0.1 mg/ml. Within 15 s a drop (5–10 μl) of diluted suspension was applied to a carbon-film-coated copper grid, the grid was rinsed with 50 μl nanopure water, partially blotted, stained by 2% uranyl acetate solution, incubated for 30 s, and finally blotted. Pipetting was done using cut tips to reduce shearing of filaments. An identical staining procedure was used for samples lacking α-actinin as for samples containing it.

The filaments were examined in a Philips (Eindhoven, The Netherlands) Tecnai-12 TEM using an acceleration voltage of 120 kV. Filament length distributions were measured manually by tracing the lengths of several hundreds of actin filaments, from approximately five micrographs taken for each time point, at different areas on the grid and from two independent experimental runs.

Lengths were measured from digitized micrographs recorded by a SIS (Münster, Germany) Megaview II charge-coupled device camera (see Fig. 1), using the SIS analySIS software. Filaments <20 nm were, in general, too short to separate from the background noise.

Depolymerization assay

We have followed the depolymerization assay described in Sagot et al. (2002) with slight modifications. Pyrene-labeled actin (10% labeled monomers) was polymerized in 0.4 × polymerization buffer, at a stock concentration of 0.15 mg/ml. Polymerization was monitored with an SLM-Aminco 8100 spectrofluorometer (Jobin Yvon, Edison, NJ) and lasted 30–40 min. Depolymerization was initiated by a short incubation with 400-nm cofilin followed by 10-fold dilution.

Samples containing α-actinin were prepared as for TEM (above). Control cuvettes were prepared identically except for adding buffer not containing α-actinin after polymerization. Samples which were depolymerized at a high KCl concentration were prepared in the same fashion except for replacing the dilution buffer to H-buffer.

Numerical analysis

Several methods have been proposed to determine the length distribution, $Pr(l)$, of linear polymers such as F-actin by analyzing the time course of depolymerization (Grazi and Trombetta, 1986; Kristofferson et al., 1980; Podolski and Steck, 1989). We will briefly describe how this can be done from the measured fluorescence intensity as a function of time, $I(t)$, obtained from a pyrene-labeled actin depolymerization assay.

Let $M(t, \Delta t)$ be the number of monomers depolymerizing in the time interval $(t, t + \Delta t)$, and let $\mathcal{I}_m$ be the loss in intensity of fluorescence at the detector per depolymerizing monomer. It follows that

$$\Delta I = I(t + \Delta t) - I(t) = -\mathcal{I}_m M(t, \Delta t). \quad (1)$$

In addition, let η be the monomer-dissociation rate and a_0 the effective monomer length in the filament. On average, by the time t, all polymers of initial length $l \le a_0\eta t$ will have completely depolymerized. In the time interval $(t, t + \Delta t)$, polymers of initial length $l \ge a_0\eta t$ will shorten by $a_0\eta\Delta t$.

To relate $I(t)$ to $Pr(l)$ we define $F(t) = Pr(l \le a_0\eta t)$ as the probability of having a filament of length $l \le a_0\eta t$, and let $\mathcal{N}_0$ be the initial number of filaments, such that

$$M(t, \Delta t) = \mathcal{N}_0\eta\Delta t(1 - F(t)). \quad (2)$$

From Eqs. 1 and 2 it follows that

$$\Delta I/\Delta t = \mathcal{I}_m\mathcal{N}_0\eta(F(t) - 1). \quad (3)$$

Because $F(t)$ is a cumulative probability function, the measured $-\Delta I/\Delta t$ is normalized to unity at $t = 0$ and to zero at $t \to \infty$. Subtracting the result from 1 yields $F(t)$. Remembering that $\Delta F(t) = F(t + \Delta t) - F(t) = Pr(a_0\eta t \le l \le a_0\eta(t + \Delta t))$ and noting that $\langle l^n \rangle = \Sigma_i (a_0\eta t_i)^n \Delta F(t_i)$, we find that both $\langle l \rangle$ and $\sigma_l = \sqrt{\langle l^2 \rangle - \langle l \rangle^2}$ are linear in the prefactors $a_0\eta$. The main point in this derivation is that although the prefactors are not all known (and are expected to change by addition of α-actinin), they cancel out when we compute the coefficient of variation, C_σ.

Since $F(t)$ is a cumulative distribution function, its relation to $I(t)$ implies that $I(t)$ should be a monotonically decreasing and convex function. The data was therefore fit nonparametrically to a smooth curve using the Dierckx algorithm for cubic spline curve fitting (Dierckx, 1980). The original

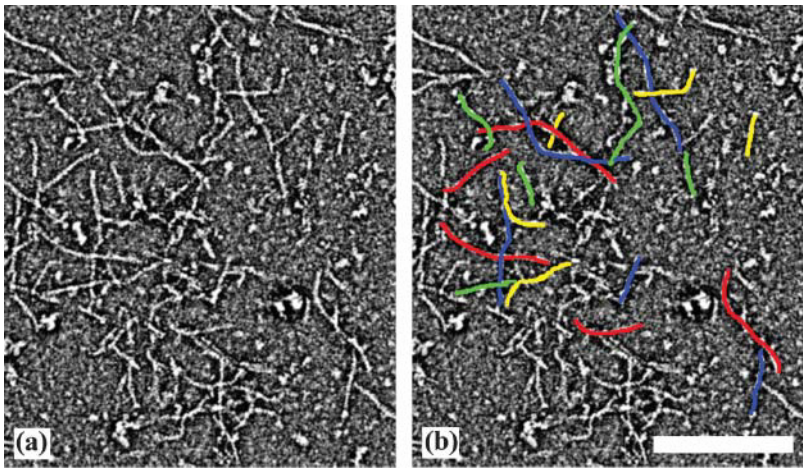

FIGURE 1 (*A*) One example of a section of a transmission electron micrograph from which F-actin length measurements were taken. The image is meant to demonstrate the quality of data from which lengths were measured. Actin was polymerized at 1.0 mg/ml and α-actinin was added when the polymerization reached a steady state. As discussed in the text, large agglomerates were disregarded. After incubating for 60 min the sample was diluted to 0.1 mg/ml and stained with 2% uranyl acetate solution. The white scale bar represents 200 nm. (*B*) An example of the manual tracing of filaments. The length of each trace was automatically computed and stored by an analySIS macro.

algorithm was modified to include monotonicity constraints in addition to its original convexity constraints.

Numerical simulation

Once polymerization has progressed until the concentration of the remaining monomers is at the critical concentration of actin, the dominating process underlying the dynamics is monomer exchange between the actin filaments and the monomer bath. The system then evolves into the steady state of this random process, in which the filament length distribution is fixed while individual filaments are still growing and shrinking. To simplify the description of filament dynamics we have used operational rate constants (Edelstein-Keshet and Ermentrout, 1998) that combine the rates of both ends in our model.

The dynamic process of monomer exchange was simulated as follows: all rates were represented by one effective dissociation rate constant. At each step two filaments were randomly chosen, and their lengths denoted l_1 and l_2. The topmost monomer was then transferred from the first filament to the second (i.e., if $l_1 > 0$ then $l_1 \rightarrow l_1 - 1$, $l_2 \rightarrow l_2 + 1$). The total number of monomers was predefined and fixed, and so was the lattice size. The maximal number of filaments could not exceed the lattice size, but the dynamics allowed formation of vacant sites that could reduce the number of polymers below the maximum.

Various initial length distributions (e.g., uniform, Gaussian, etc.) were found to produce similar steady-state distributions (the difference being only in the transient behaviors). A sweep was defined to be a number of monomer-exchange steps equal to the total number of monomers (1200–3000, divided between 30–100 filaments). At the end of each sweep the average filament length and the variance of the distribution were recorded. The distribution reached a steady state typically after a few hundred sweeps (in extreme cases the transient persisted for up to 1000 sweeps). A typical simulation was run for 400–500 sweeps and C_σ was averaged over the final 200 sweeps.

The effect of crosslinkers was modeled by reducing the dissociation rate of pairs of crosslinked monomers from different filaments. Filament pairs were chosen at random, and not necessarily from adjacent sites on the lattice (since the lattice site indices were not assumed to represent the spatial positions of real filaments in a three-dimensional solution).

The topmost monomer of the shorter polymer was crosslinked to a monomer at the same position on the longer filament (e.g., monomer number 10 of a length-10 polymer was crosslinked to monomer number 10 of a length $\geq$10 polymer). Each polymer pair could have at most one crosslink. Filaments were allowed to grow on top of a crosslinked monomer, thereby pushing the link down from the topmost position. The model is a simple description of multiple crosslinks as ladder rungs. Only the links closest to the edge (top rung) can affect the monomer-exchange dynamics.

If a monomer dissociated then all the crosslinks that originated from it were deleted. Crosslinkers eliminated in this fashion were moved to new positions randomly chosen. The effective dissociation rate of crosslinked monomers was an independent parameter of the model. Slight variations of the model (e.g., crosslinking random monomers within the filament, crosslinking only adjacent filaments on the lattice, etc.) did not alter the observed characteristics of the steady-state distribution.

RESULTS

Experimental

Analysis of data from TEM

We first measured the length distribution from digitized TEM images of F-actin and of gelsolin-capped F-actin in the absence of crosslinks. These distributions were indeed exponential, characterized by $C_\sigma \approx 1$ (data not shown inasmuch as they reproduce previous results; see Janmey et al., 1986; Burlacu et al., 1992). The average polymer length was a decreasing function of gelsolin concentration at a fixed actin concentration.

The gelsolin concentration in our experiment corresponds to 80 monomers of actin per filament, which are known to extend ~210–220 nm. In the measurements described, the actual mean filament length is also affected by the amount of active actin and gelsolin protein in the solution, and was measured to be 161 $\pm$ 15 nm. We attribute the deviation from the predicted average length to uncertainty in the amount of active protein and to possible shearing of the filaments during transfer to the TEM.

Addition of α-actinin (without stabilization by phalloidin) changes the distribution of lengths: the presence of crosslinks reduces σ_1 by two- to threefold for a given $\langle l \rangle$. Fig. 2 represents our main result, showing the measured length distribution at different time points beginning shortly after adding α-actinin to a solution of F-actin. The initial width of the distribution is $\sigma_{t=0} \approx \langle l \rangle$, and it reduces in time until $\sigma_{t=60} \approx \langle l \rangle / 2.5$.

We simulated numerically the effect of random shearing on C_σ and found that it is in the 10–20% range. This was done by generating an exponential length distribution, breaking each element at random locations and comparing the results with those obtained for several narrower distributions. In addition, previous work has shown a good agreement between the values of C_σ measured by TEM and fluorescent optical microscopy (without crosslinkers), with both methods giving values close to unity (Janmey et al., 1986; Burlacu et al., 1992). We also could not obtain length distributions from filaments inside of large agglomerates. The filaments we do measure were probably mostly separated or broken off from bundles during the sample preparation, but this cannot decrease C_σ by a factor of two for the reasons stated above. We conclude therefore that our observation of twofold (or larger) changes in the coefficient of variation of the distribution is not due to artifacts of the TEM measurement.

Analysis of data from actin depolymerization assays

Fig. 3 presents data from an actin depolymerization assay in the absence and in the presence of α-actinin. We have analyzed a total of 36 experiments: 14 depolymerized at normal KCl concentration (six with α-actinin and eight without) and 22 at a high KCl concentration (12 with α-actinin and 10 without). Two measurements can be obtained from this assay. The first is the functional form of the fluorescence intensity, and the second is the decay time for the fluorescence. As we shall see, each of these yields a different characterization of the length distribution of actin filaments (which was previously measured in the TEM).

We first extracted C_σ from the monotonic and convex fit to $I(t)$ (see Materials and Methods). Since C_σ is calculated from the second derivative of $I(t)$, it is sensitive to noise. From the data obtained at 50 mM KCl we found that without α-actinin, $\langle C_\sigma \rangle = 1.6 \pm 0.2$ and with α-actinin, $\langle C_\sigma^\alpha \rangle = 1.0 \pm 0.2$

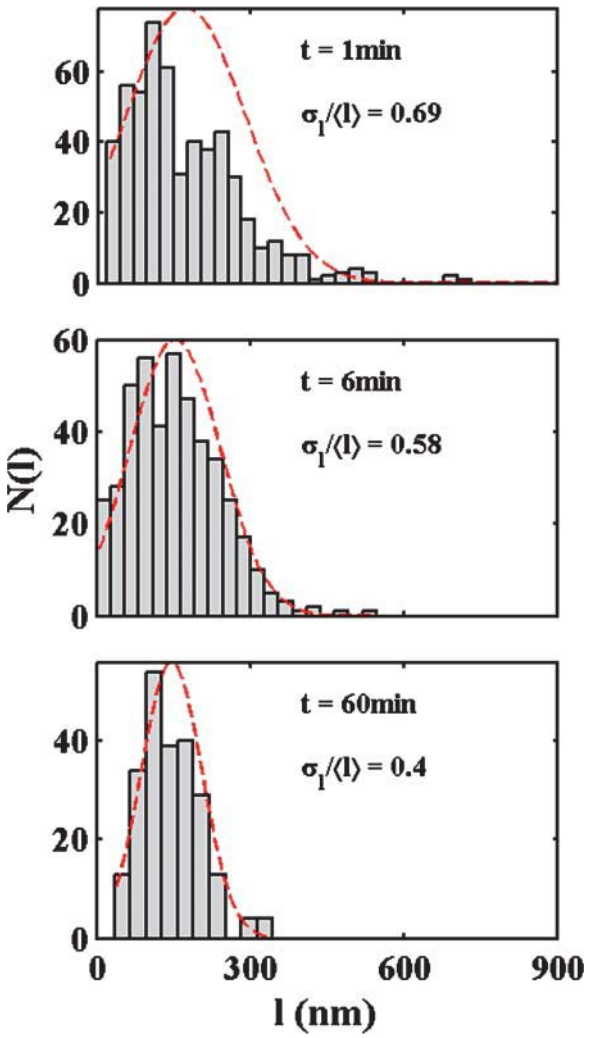

FIGURE 2 Time evolution of actin filament length distribution as measured from transmission electron micrographs. Actin filaments were polymerized in the presence of gelsolin. At $t = 0$ min α-actinin was added. The distributions shown were measured from samples taken at $t = 1$ (540 filaments from seven micrographs), $t = 6$ (421 filaments from six micrographs), and $t = 60$ min (231 filaments from three micrographs). The three distributions yielded $C_\sigma = 0.69$, 0.58, and 0.40, respectively. The dotted lines represent Gaussian distributions with mean and variance according to the measured values. These are given only as a guide to the eye (the actual distributions are not expected to be Gaussian).

(where the errors are statistical, i.e., originate from the variance between experiments). The effect of noise in the high salt concentration experiments was too great to yield meaningful results.

The fluorescence data confirms that the length distribution in the presence of α-actinin is narrower than the distribution of F-actin alone, but does not reproduce the precise values $C_\sigma = \sim 1$ and $C_\sigma^\alpha = \sim 0.4$ obtained from the TEM, giving instead double the value for both cases. To explain this we investigated numerically the effect of noise on the measured values of C_σ. We did this by constructing model intensity curves that would reproduce length distributions with $0.3 \leq C_\sigma \leq 1$ when subjected to the method of analysis we have used on our fluorescence data. We then added to them different levels of (white) noise, and analyzed the resulting noisy curves. We found that the resulting value of C_σ is indeed sensitive to noise—i.e., moderate levels of additive white noise (an amplitude $\leq 10\%$ of the signal) can increase C_σ twofold. The important point is that this happens in a similar way for different C_σ, preserving their ratio.

We also calculated the average decay time, $\tau_{1/2}$, that it took the fluorescence to reach one-half of its initial value (See Fig. 4). Decay times from different experimental conditions were found to be statistically separable despite a large variability. We shall now show that the values of $\tau_{1/2}$ that we measured are consistent with our TEM results, based on the observation that $\tau_{1/2}$ is determined by two competing effects that exist in our experiment: it increases when the average time for monomer dissociation (τ_{md}) increases, but decreases when the variance of length decreases.

The first effect is an intuitive one: a local stabilization of the actin filament by α-actinin will increase τ_{md} and hence also $\tau_{1/2}$. A binding energy excess of $\gamma k_{\mathrm{B}}T$ associated with a monomer bound to a crosslinker will thus lead to a longer dissociation time when compared to a monomer which is not bound.

However, for a given average filament length, a reduced coefficient of variation (C_σ) implies a narrow distribution. This will increase the number of simultaneously active depolymerization sites, and hence decrease $\tau_{1/2}$. An extreme example is an ensemble of filaments with the same length, $\langle l \rangle$. At each time interval every one of the filaments will shorten by $a_0\eta\Delta t$, and depolymerization will proceed linearly with the shortest possible $\tau_{1/2} = \langle l \rangle / 2a_0\eta$.

We have also simulated $\tau_{1/2}$ numerically (the time it takes one-half of the monomers to depolymerize) in a model where each surviving filament shrinks at a constant rate. Comparing an initial exponential length distribution to several initial distributions with the same mean but smaller standard deviation we find that reducing C_σ by a factor of 2–3 will also reduce $\tau_{1/2}$ by a factor of 2–3.

We have measured the ratio $r = \tau_{1/2}/\tau_{1/2}^\alpha$ to be $r_{50\ \mathrm{mM}} = 2.8 \pm 1.2$ for depolymerization at 50 mM KCl, and $r_{1\mathrm{M}} = 1.9 \pm 0.7$ for depolymerization at 1 M KCl. The small salt dependence is attributed to the change in the binding strength of the crosslinker. A stronger bond in high salt concentration is consistent with the evidence suggesting that a hydrophobic interaction plays an important role in the actin α-actinin interaction (Miyata et al., 1996), but in our experiment this effect is weaker than the noise.

These results indicate that the increase in τ_{md} is small, and the dominating effect is the speedup due to the smaller C_σ. This is consistent with the weak bond between actin and α-actinin, and the fact that only part of its energy contributes to stabilize a given monomer. As we discuss in the section Theoretical, below, we have constructed a model and found that theoretically a weak ($\gamma \simeq 1\ k_{\mathrm{B}}T$) stabilizing effect can reduce C_σ two- to threefold.

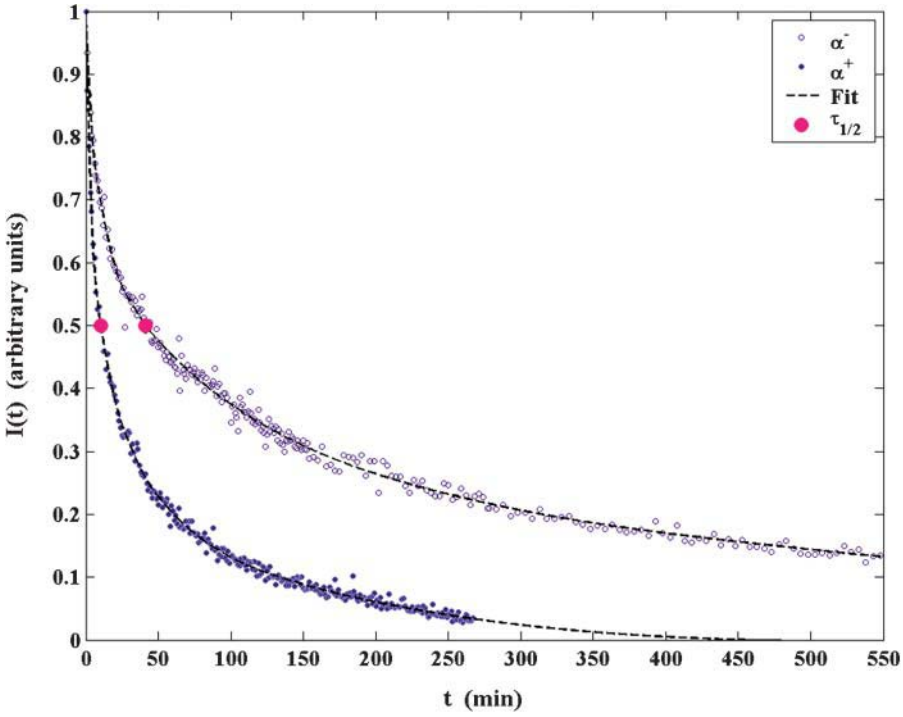

FIGURE 3 Normalized fluorescence decay curves of depolymerizing pyrene-labeled F-actin (10% labeled monomers). (○) Depolymerization of F-actin without α-actinin; (●) depolymerization of crosslinked filaments. The dashed line represents a monotonic and convex nonparametric least-square fit to the experimental data. The second derivative of this fit enables us to calculate C_σ, as explained in the text. The large circles are located at the times when the fluorescence intensity reached one-half of its initial value ($\tau_{1/2}$).

Theoretical

Exponential distribution in the absence of crosslinkers is a manifestation of a zero-range process

The dynamics of actin polymerization and depolymerization in the absence of crosslinkers has been mathematically modeled by others, and was theoretically shown to yield a steady-state exponential length distribution (Edelstein-Keshet and Ermentrout, 1998). However, it is insightful to view the exponential distribution in the context of a more general theoretical framework, namely the framework of zero-range processes.

A zero-range process takes place on a one-dimensional lattice, with $\mathcal{P}$ sites (each nonempty lattice site refers to

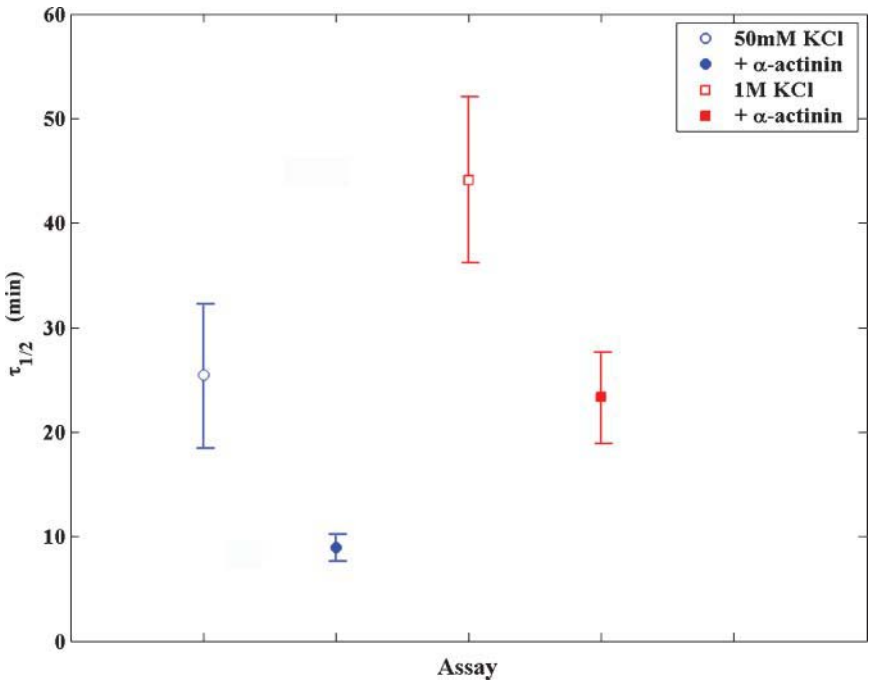

FIGURE 4 The time it took for the fluorescence intensity to reach one-half of its initial value ($\tau_{1/2}$) in four depolymerization assays. (○) F-actin in 50 mM KCl (averaged over eight assays); (●) F-actin crosslinked by α-actinin in 50 mM KCl (averaged over six assays); □, F-actin in 1*M* KCl (averaged over 10 assays); and ■, crosslinked F-actin in 1 M KCl (averaged over 12 assays). These timescales can be effected by both the monomer-dissociation rate and by C_σ. The dominant effect in our experimental conditions is the speeding up due to C_σ.

a single polymer). The length of a polymer at site $1 \leq \mu \leq \mathcal{P}$ is denoted l_μ. The total number of indistinguishable monomers, $\mathcal{M} = \sum_\mu l_\mu$, is conserved. A zero-range process is homogeneous if its monomer-dissociation and -association rates are space -independent. It was shown in Evans (2000) that the homogeneous zero-range process yields an exponential length distribution,

$$Pr\{l_\mu\} \sim e^{-l_\mu/\lambda}, \tag{4}$$

where λ is the mean of the distribution (and a very good approximation to the average filament length, $\langle l \rangle$, for $\langle l \rangle \gg 1$).

Using typical values for the critical concentration of actin (0.1 mg/ml) and its diffusion constant (100 μm/s^2) one can estimate that the average distance between actin monomers in a solution of F-actin is ~50–100 nm, and the diffusion timescale is ~100 μs. Actin polymerization and depolymerization timescales, on the other hand, are typically on the order of 0.1–1 s. This separation in timescales justifies the assumption that exchanging monomers is much slower than diffusion, i.e., the solution (which is at the critical monomer concentration) is spatially independent and the process is homogeneous.

Modeling monomer exchange

From the theoretical point of view locally stabilizing crosslinks excludes the monomer dynamics from the class of zero-range processes, since a situation where all the dissociation rates are preset and unaffected by the dynamics no longer exists. Simulating monomer exchange in the presence of randomly placed stabilizing links results in the variance dropping two- to threefold (depending on parameter values). An explicit example is shown in Fig. 5 *A*.

The probability of dissociation of a crosslinked monomer is a key parameter in the model, and it depends exponentially on the actin-actinin bond energy excess, γ. However, the uncertainty in the experimental value of γ is rather large (Miyata et al., 1996). To estimate the effect that changing γ would have on C_σ we ran our simulation, changing the excess binding energy of a crosslinked monomer in the range of $0 < \gamma < 5\ k_BT$. The results are shown in Fig. 5 *B*. We conclude that in our model $C_\sigma(0)/C_\sigma(\gamma) \approx 2$–3 for $0.5 < \gamma < 5\ k_BT$.

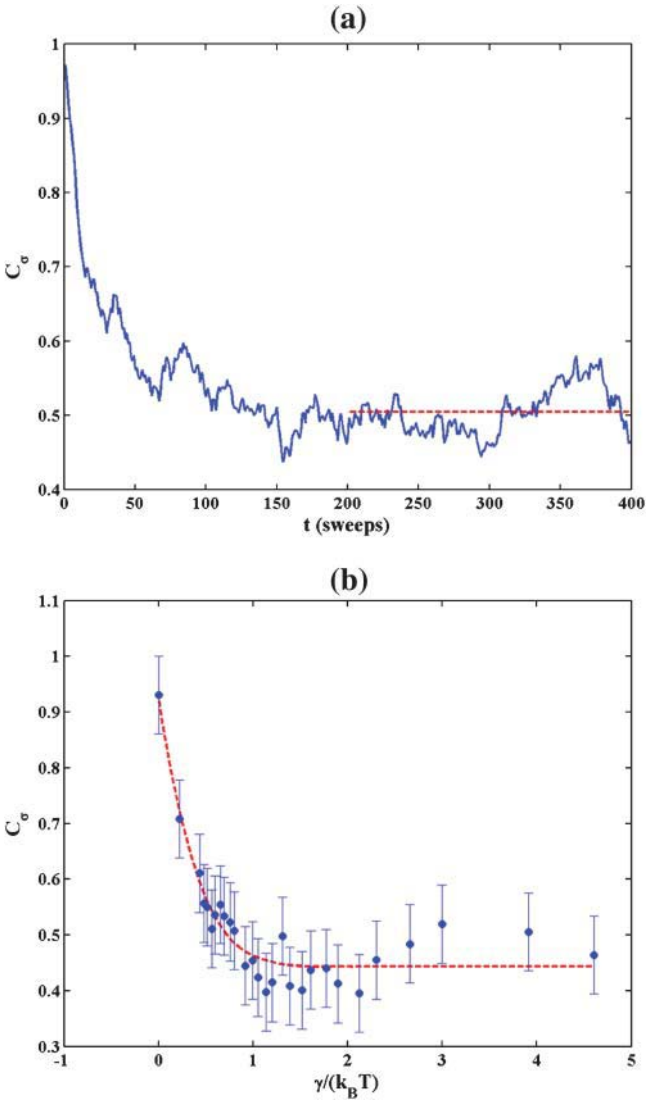

FIGURE 5 Results from simulating a monomer-exchange process. (*A*) Time evolution of C_σ in a monomer-exchange simulation. The simulation presented consisted of 10,000 monomers divided among 200 nucleation sites, so that the mean length was approximately fixed at the value of 50 monomers. 10% of the filament pairs were crosslinked, and the crosslink bond energy excess is $\gamma = 1\ k_BT$. The initial filament length distribution was exponential. Time is measured in simulation sweeps. We obtain here $\langle C_\sigma \rangle = 0.505$ after averaging over the final 200 sweeps (*dashed line*). (*B*) The coefficient of variation, C_σ, as a function of the crosslink bond energy excess, γ. Each data point represents the average of the values obtained from three independent simulations with 1200 monomers and 40 nucleation sites that were run for 400 sweeps. The dashed line is a monotonic least-square fit.

DISCUSSION

Within our theoretical model the interplay between stabilizing monomer pairs and narrowing length distribution formally originates from the exclusion of the monomer-exchange dynamics from the class of zero-range processes. If crosslinked monomers are harder to dissociate, then portions of a filament which overlap a crosslinked neighbor will be more stable. A smaller variance of lengths is the basic manifestation of this statistical tendency to overlap. Hence, crosslinks that reduce the monomer-dissociation rate will also increase the uniformity of filament lengths.

In a structure of elastic filaments such as the actin cortex of the cytoskeleton, filaments that are much shorter or much longer than the average will fail to contribute their share to the strength of the construction. This is even more applicable

in the case of a dynamic structure such as the contractile ring. Such considerations seem to be borne out experimentally in the actin contractile ring, where filament sizes are mostly in the range of several hundred nanometers (Schroeder, 1972, 1990).

In summary, we have shown that α-actinin reduces the variation in actin filament lengths in vitro by comparing TEM and fluorescence measurements from samples with crosslinkers to samples without them. The two types of samples have consistently been found to be distinguishable. Our measurements are consistent with the assumption that α-actinin induces a weak local stabilization of crosslinked monomer pairs from different actin filaments. The reduction in C_σ is robust in the sense that the qualitative effect of the crosslinker does not depend upon specific structure, and can thus be thought of as a general mechanism for regulating the variance of the steady-state length distribution of monomer-exchanging linear filaments.

We thank C. Storm, F. MacKintosh, and M.-F. Carlier for useful discussions.

This investigation was supported in part by the Binational Science Foundation under grant #2000298, and by the MINERVA Foundation, Munich, Germany.

REFERENCES

Allen, P. G., C. Shuster, J. Käs, C. Chaponnier, P. A. Janmey, and I. Herman. 1996. Phalloidin binding and rheological differences among different actin isoforms. *Biochemistry*. 35:34–38.

Burlacu, S., P. A. Janmey, and J. Borejdo. 1992. Distribution of actin filament lengths measured by fluorescence microscopy. *Am. J. Physiol.* 262:C569–C577.

Dierckx, P. 1980. An algorithm for cubic spline fitting with convexity constraints. *Computing*. 24:349–371.

Edelstein-Keshet, L., and G. B. Ermentrout. 1998. Models for the length distributions of actin filaments. I. Simple polymerization and fragmentation. *Bull. Math. Biol.* 60:449–475.

Evans, M. R. 2000. Phase transitions in one-dimensional nonequilibrium systems. *Braz. J. Phys.* 30:42–57.

Grazi, E., and G. Trombetta. 1986. Evaluation of the actin filament length from the time course of the depolymerization process. *Biochem. Biophys. Res. Comm.* 139:109–114.

Janmey, P. A., J. Peetermans, K. S. Zaner, T. P. Stossel, and T. Tanaka. 1986. Structure and mobility of actin filaments as measured by quasielastic light scattering, viscometry and electron microscopy. *J. Biol. Chem.* 261:8357–8362.

Janmey, P. A., S. Hvidt, J. Käs, D. Lerche, A. Maggs, E. Sackmann, M. Schliwa, and T. P. Stossel. 1994. The mechanical properties of actin. *J. Biol. Chem.* 269:32503–32513.

Kreis, T., and R. Vale. editors. 1999. Guidebook to the Cytoskeletal and Motor Proteins, 2nd Ed. Oxford University Press, New York.

Kristofferson, D., T. L. Karr, and D. L. Purich. 1980. Dynamics of linear protein polymer disassembly. *J. Biol. Chem.* 255:8567–8572.

Littlefield, R., and V. M. Fowler. 1998. Defining actin filament length in striated muscle: rulers and caps or dynamic stability? *Annu. Rev. Cell Dev. Biol.* 14:487–525.

McGough, A., M. Way, and D. DeRosier. 1994. Determination of the alpha-actinin-binding site on actin filaments by cryoelectron microscopy and image analysis. *J. Cell Biol.* 126:433–443.

Miyata, H., R. Yasuda, and K. Kinosita, Jr. 1996. Strength and lifetime of the bond between actin and skeletal muscle α-actinin studied with an optical trapping technique. *Biochim. Biophys. Acta.* 1290:83–88.

Newman, J., K. S. Zaner, K. L. Schick, L. C. Gershman, L. A. Selden, H. J. Kinosian, J. L. Travis, and J. E. Estes. 1993. Nucleotide exchange and rheometric studies with F-actin prepared from ATP- or ADP-monomeric actin. *Biophys. J.* 64:1559–1566.

Piekenbrock, T., and E. Sackmann. 1992. Quasielastic light scattering study of thermal excitations of F-actin solutions and of growth kinetics of actin filaments. *Biopolymers*. 32:1471–1489.

Podolski, J. L., and T. L. Steck. 1989. Length distribution of F-actin in *Dictyostelium discoideum*. *J. Biol. Chem.* 265:1312–1318.

Ruddies, R., W. H. Goldman, G. Isenberg, and E. Sackmann. 1993. The viscoelasticity of entangled actin networks: the influence of defects and modulation by talin and vinculin. *Eur. Biophys. J.* 22:309–312.

Sagot, I., A. A. Rodal, J. Moseley, B. L. Goode, and D. Pellman. 2002. An actin nucleation mechanism mediated by Bni-1 and Profilin. *Nat. Cell Biol.* 4:626–631.

Schroeder, T. E. 1972. The contractile ring. II. Determining its brief existence, volumetric changes, and vital role in cleaving *Arbacia* eggs. *J. Cell. Biol.* 53:419–434.

Schroeder, T. E. 1990. The contractile ring and furrowing in dividing cells. *Ann. N. Y. Acad. Sci.* 582:78–87.

Xu, J., W. H. Schwartz, J. A. Käs, T. P. Stossel, P. A. Janmey, and T. D. Pollard. 1998. Mechanical properties of actin filament networks depend on preparation, polymerization conditions, and storage of actin monomers. *Biophys. J.* 74:2731–2740.

Xu, J., J. F. Casella, and T. D. Pollard. 1999. Effect of capping protein, CapZ, on the length of actin filaments and mechanical properties of actin filament network. *Cell Motil. Cytoskeleton.* 42:73–81.

Yin, H. L. 1999. Gelsolin. *In* Guidebook to the Cytoskeletal and Motor Proteins, 2nd Ed. T. Kreis and R. Vale, editors. Oxford University Press, San Francisco, CA. 99–102.